

# Chapter 1

## Introduction

### *1.1 Multiband OFDM – a background*

In February 2002, Federal Communications Commission (FCC) allocated 7500 MHz of spectrum for unlicensed use of ultra wideband (UWB) devices for communication applications in the 3.1–10.6-GHz frequency band [FCC02], opening up a new application area for very high bandwidth short range wireless systems. FCC defines UWB as any signal that occupies more than 500 MHz bandwidth in the allocated band and meets the maximum average output power spectral density (PSD) of  $-41.3$  dBm/MHz. However the concept of UWB has its origins in the 1960s when it was used for sending low duty cycle bursts of RF signal for various applications ranging from ground-penetrating radars to jamming resistant impulse radios utilizing pulse position modulation. Impulse radios suffer from two severe disadvantages, limiting their usefulness for consumer applications:

- a) The available data rate is not limited by the width of the pulses, but rather due to the inter-pulse spacing, which needs to be sufficiently large to ensure that even after delay spread, the pulses do not substantially overlap.
- b) The requirement of sub nanosecond pulses and high resolution receivers pose considerable circuit design challenges.

This required exploration of new transmission technologies, resulting in the eventual emergence of two competing candidates: Multiband OFDM (MBOFDM) and Direct Sequence UWB [Batra04]. Multiband OFDM has been finally standardized as the physical layer of choice by ECMA [ECMA368]. Because of the high bandwidth available, UWB transmitters are capable of:

- a) Coexisting with other services in the same frequency band without significantly affecting the performance of narrowband services (which would typically transmit with a much higher

power spectral density) as well as other UWB radios. This allows for convenient unlicensed parasitic operation.

- b) Precision distance/positioning/ranging measurements during the course of normal data transmission-reception.

However the requirement for coexistence presents a serious challenge to design of any UWB receiver because of the low signal to noise ratio environment in which the receiver needs to operate and the possibility of narrowband interferers which may be stronger than the desired signal itself.

## ***1.2 Overview of ECMA 368 standard for Multiband OFDM***

In Multiband OFDM (MBOFDM) modems following the ECMA-368 standard [ECMA368], the transmitter may hop across 3 adjacent bands, over a bandwidth of  $528\text{MHz} * 3 = 1584\text{MHz}$ . Fast hopping requires that there be some silent period between two OFDM symbols, thus necessitating the use of zero padded suffix (ZPS) at the end of every OFDM symbol, instead of the more common method of pre-appending a cyclic prefix. While the hopping sequence is communicated by the MAC, the exact hopping instant is not known to the remote receiver. Thus the transmitted signal will be received partially till timing synchronization is complete; making it difficult to employ any data aided timing acquisition method. Further, this timing acquisition needs to be carried out in presence of delay spread which may potentially go up to 19.4% of OFDM symbol duration [Foerster02], flattening out any correlation/early-late gate based acquisition metrics, reducing the reliability of data aided timing acquisition processes.

To enable reliable clock frequency correction with a simple linear interpolator and a slip detector, sufficient oversampling factor is required. In subsequent sections, an oversampling factor of  $N_{ov}$  has been used to describe the acquisition and estimation scheme, though the only practically realizable value of  $N_{ov}$  would be 2, requiring the Analog to Digital Converters (ADC) to run at 1056MSPs.

The frame structure of an ECMA 368 Multiband OFDM packet is shown in Fig 1.1.

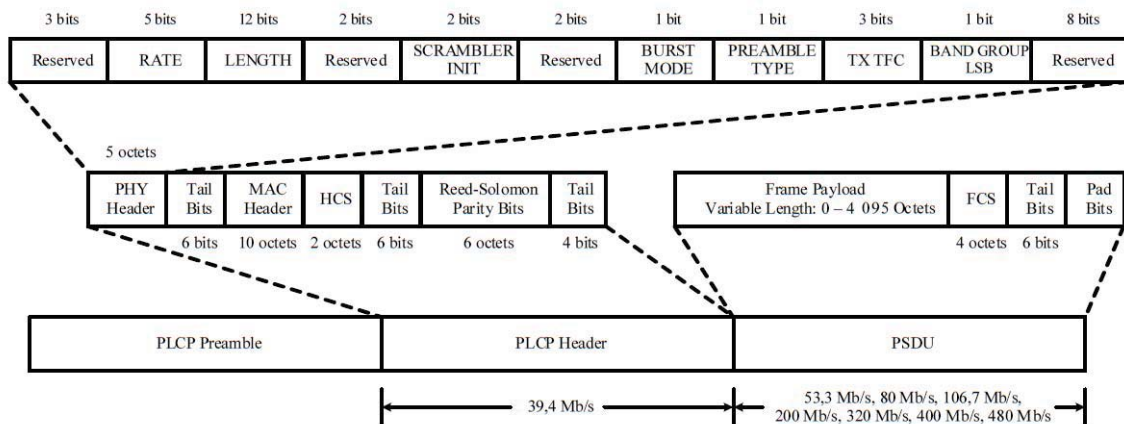


Figure 1.1: Frame structure of a Multiband OFDM packet.

A Multiband OFDM packet consists of a known preamble pre-appended to the payload to aid synchronization, channel frequency response estimation and correction of the frequency offset between the transmitter and receiver. The preamble (9.375  $\mu$ s) is a real baseband signal and is unique to the Time-Frequency Code (TF Code). The preamble has two parts: a 7.5  $\mu$ s long Time Domain Sequence (TDS) and a 1.875  $\mu$ s long Frequency Domain Sequence (FDS). The time domain sequence is constructed as follows: For a given TF code, the appropriate base TDS  $s_{base}[l]$  is selected from Tables 4 -10 and the appropriate Standard cover sequence  $s_{cover}[m]$  from Table 21 of [ECMA368]. To make the structure of each preamble unit similar to that of the payload OFDM symbol  $s_{base}[l]$  is extended in time-domain sequence by appending the zero padded suffix to create  $s_{ext}[l]$ . Finally the  $k$ th sample of the  $n$ th symbol in the Standard preamble  $s_{sync}[n,k]$ , corresponding to TDS is given by  $s_{sync}[n,k] = s_{cover}[n] \times s_{ext}[k]$ . The channel estimation sequence or FDS is also constructed in a similar fashion. A base channel estimation sequence  $s_{est}[l]$  is created by taking the inverse discrete Fourier transform (IDFT) of the frequency-domain sequence defined in Table 23 of [ECMA368] and appending a zero-padded suffix to the resulting time-domain output. The channel estimation sequence portion of the Standard preamble is created by successively appending 6 periods of the base estimation sequence, or equivalently, spreading the base channel estimation sequence with a sequence of [1 1 1 1 1 1]. Both TDS and FDS need to be normalized to ensure that the average power of the preamble is same as that of the payload. The TDS or the packet/frame synchronization sequence can be used for packet acquisition and detection, coarse carrier frequency estimation, coarse

symbol timing, and for synchronization within the preamble. The FDS or the channel estimation sequence can be used for estimation of the channel frequency response, fine carrier frequency estimation, and fine symbol timing. The first sample of the first channel estimation symbol is used as the timing reference point for range measurements.

A packet header is added after the preamble to convey information about both the PHY and the MAC that is needed at the receiver in order to successfully decode the information symbols. The scrambled and Reed-Solomon encoded PHY header is constructed in the following fashion:

1. Formatted PHY header is created based on the information provided by the MAC.
2. The Header Checksum value (HCS), spanning over 2 octets is computed over the combined PHY and MAC headers and appended to the MAC header. The resulting combination (MAC Header + HCS) is scrambled according to Section 10.5 of [ECMA368]. This is protected using a shortened Reed-Solomon code (23,17)
3. 6 tail bits are inserted after the PHY header, 6 tail bits after the scrambled MAC header and HCS, and 6 parity octets and 4 tail bits at the end to form the scrambled and Reed-Solomon encoded header.

The resulting scrambled and Reed-Solomon encoded header is encoded, using a  $R = 1/3$ ,  $K = 7$  convolutional code, interleaved using a bit interleaver, mapped onto a QPSK constellation and finally mapped to the appropriate data subcarriers. The PHY header contains information about the data rate of the MAC frame body, the length of the frame payload (which does not include the FCS), the seed identifier for the data scrambler, and information about the next packet – whether it is being sent in burst mode and whether it employs a burst preamble or not. The PHY header field is composed of 40 bits, numbered from 0 to 39. Bits 3-7 encode the RATE field, which conveys the information about the type of modulation, the coding rate, and the spreading factor used to transmit the MAC frame body. Bits 8-19 encode the LENGTH field, with the least-significant bit being transmitted first. Bits 22-23 encode the seed value for the initial state of the scrambler, which is used to synchronize the descrambler of the receiver. Bit 26 encodes whether or not the packet is being transmitted in burst mode. Bit 27 encodes the preamble type (Standard or burst preamble) used in the next packet if in burst mode. Bits 28-30 is used to indicate the lower 3 LSBs of the TFC (T1 - T3) used at the transmitter. Bit 31 indicates the LSB

of the band group used at the transmitter. Bit 34 indicates the MSB of the TFC (T4) used at the transmitter. All other bits are reserved for future use and are to ZERO. The receiver cannot assume that reserved bits are ZERO on receive, for instance to assist the Viterbi algorithm or to decode the RATE quickly.

The payload bit-stream is constructed as defined by starting with the non-scrambled data bits received from the MAC, appending the frame payload with the 4-octet Frame Check Sequence (FCS), 6 tail bits, and a sufficient number of pad bits in order to ensure that the payload is aligned on the interleaver boundary. The resulting combination is scrambled and the six tail bits in the scrambled stream are replaced with 6 “ZERO” bits. This is encoded, as defined, using a  $R = 1/3$ ,  $K = 7$  convolution code and punctured to achieve the appropriate coding rate, interleaved using a bit interleaver, mapped onto either a QPSK or DCM constellation (defined subsequently), and mapped to the data subcarriers in order to create the OFDM symbols.

For the 8 different payload data-rates supported in the standard, three different modulation/diversity schemes are used. This is illustrated in Table 1.1. In case of Dual Carrier Modulation (DCM), two 16-QAM like constellations (bearing same information) are transmitted on subcarriers that are spaced 50 apart. In case of DCM, the coded and interleaved binary serial input data,  $b[i]$  ( $i = 0, 1, 2, \dots$ ) is divided into groups of 200 bits and converted into 100 complex numbers as follows: The 200 coded bits are grouped into 50 groups of 4 bits. Each group is represented as  $(b[g(k)], b[g(k)+1], b[g(k) + 50], b[g(k) + 51])$ , where  $0 \leq k < 50$  and  $g(k) = 2k, k < 25$  and  $2k+50$  otherwise. Each group of 4 bits  $(b[g(k)], b[g(k)+1], b[g(k) + 50], b[g(k) + 51])$  are mapped onto a four-dimensional constellation, as defined in Figure 1.2, and converted into two complex numbers  $(d[k], d[k + 50])$ . The complex numbers is normalized before mapping onto the data subcarriers.

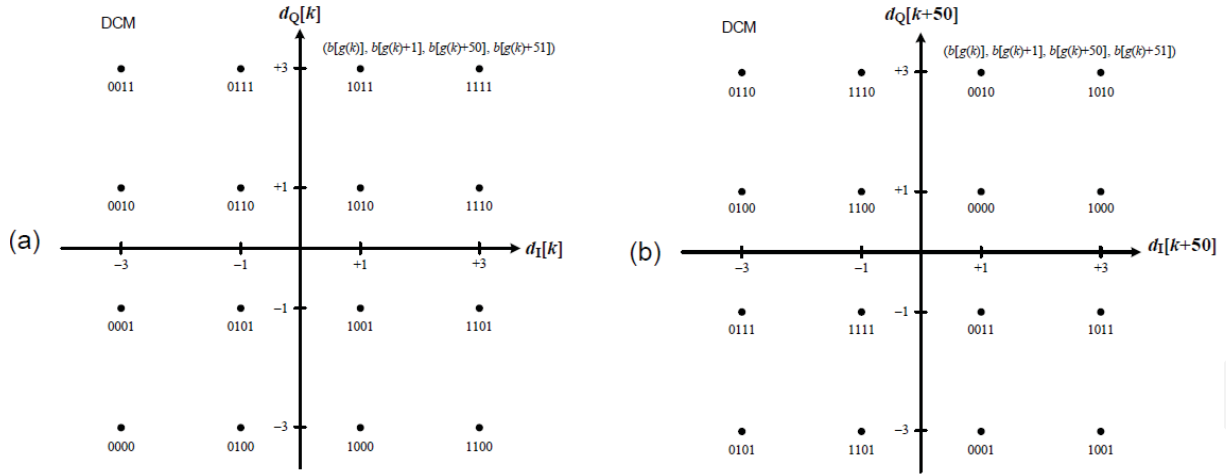


Figure 1.2: Constellation map for DCM

Table 1.1: Modulation schemes in Multiband OFDM

Data Rate (Mb/s)	Modulation	Time Spread Factor	Spreading Gain	Coded bits / OFDM symbol
53.3	QPSK	2	4	100
80	QPSK	2	4	100
106.7	QPSK	2	2	200
160	QPSK	2	2	200
200	QPSK	2	2	200
320	DCM	1	2	200
400	DCM	1	2	200
480	DCM	1	2	200

In each OFDM symbol, out of the 128 available subcarriers 122 are used while the subcarriers at the edge and at DC are nulled to conform to the spectral mask requirements. Out of these 122, 100 bear payload symbols, 10 are pilots and the rest 12 are guard subcarriers, which can be nulled or used for repeating any of the payload symbols. Within the OFDM modulation process, frequency-domain spreading within a symbol and time-domain spreading across two

consecutive symbols is used to obtain further bandwidth expansion, beyond that provided by the forward error correction code and the time-frequency codes. Frequency-domain spreading entails transmitting the same information (complex number) on two separate subcarriers within the same OFDM symbol. Time-domain spreading involves transmitting the same information across two consecutive OFDM symbols. This technique is used to maximize frequency-diversity and to improve the performance in the presence of other non-coordinated devices.

For each OFDM symbol, starting with the channel estimation sequence, there are ten guard subcarriers, 5 on each edge of the occupied frequency band. The relationship between the power levels of the guard subcarriers and that of the data subcarriers may vary across different implementations, but should remain constant within a packet, i.e., from the start of the channel estimation sequence to the end of the packet. In addition, the power levels for the guard subcarriers should be chosen to ensure that the transmitted signal meets the local regulatory requirements of minimum occupied bandwidth and spectral mask. The 10 guard subcarriers are located on either edge of the OFDM symbol; the data on these are created by copying over the five outermost data-bearing subcarriers from the nearest edge of the OFDM symbol. This provides an extra measure of diversity for the edge data subcarriers which are usually hit hardest when the coherence bandwidth of the channel is significantly less than the OFDM symbol bandwidth.

In all of the OFDM symbols following the preamble, twelve subcarriers are dedicated to pilot signals in order to allow for coherent detection and to provide robustness against frequency offsets and phase noise. These pilot signals are placed in logical frequency subcarriers -55, -45, -35, -25, -15, -5, 5, 15, 25, 35, 45, and 55. The mapping between actual pilot sequence and the pilot subcarriers is dependent on the data portion of the Payload and the data rate and are defined in Sections 10.104.1-4 of [ECMA368].

### ***1.3 Objectives of the thesis***

Multiband transmission and fast hopping in MBOFDM allows efficient use of the available UWB spectrum without prohibitive increase in hardware complexity [Batra03], [Aiello03]. Since the transmitter can hop across three bands, the PSD in each band can be increased by an 3 times without violating the overall spectral emission limitations imposed by FCC. Orthogonal frequency division multiplexing (OFDM) on the other hand allows easy capture of the available multipath energy by splitting up the high bit rate stream into multiple parallel low bit rate streams, each of which would suffer from flat fading[Nee00]. OFDM also allows easy suppression of transmission in portions of the spectrum where narrowband victim services need to be provided with extra protection.

MBOFDM or its variants are thus expected to become the technology of choice in high bandwidth short range wireless links between various consumer and computing devices replacing the traditional cable/bus connections for the same, for example in Wireless USB/Wireless Firewire etc. That is why detailed study of baseband receiver design for an MBOFDM system and exploration of different mechanisms to hence the transmission efficiency of MBOFDM frames is of current relevance.

### ***1.4 Contributions of the thesis***

In this thesis, the focus is on the study of various aspects of MBOFDM transmission and reception including the following areas:

- a) Design a baseband receiver for MBOFDM that can efficiently handle the large delay spread encountered for a signal of bandwidth 528 MHz.
- b) Explore mechanisms to improve robustness of the above receiver to IQ mismatch.
- c) Explore mechanisms to enhance the data rate and transmission efficiency of a MBOFDM transmitter beyond what is currently available in [ECMA368].



- d) Develop an analytical framework for the problem of detection of narrow band interferers with the MBOFDM receiver.

### ***1.5 Organization of the thesis***

A brief survey of available literature on various issues related to design of a MBOFDM link is presented in Chapter 2.

Chapter 3 describes the overall structure for the MBOFDM baseband receiver following the transmission scheme laid down in [ECMA368]. Robust algorithms for timing synchronization, carrier/clock frequency offset estimation and correction that can handle the requirement of low SNR and high multipath are also proposed in this chapter. The proposals are validated through extensive performance studies, both through simulation as well as analytical formulation. The effects of subcarrier nulls as defined in Section 9.2 of [ECMA368] on the timing acquisition are examined and an alternate method is proposed that does not rely on knowledge of the preamble symbols. An alternate construction of the preamble in an MBOFDM burst that can enhance the reliability of timing acquisition is also proposed in Chapter 3. This is followed by a brief description of a scheme to initialize an MBOFDM receiver without prior knowledge of the hopping sequence. Though [ECMA368] mandates the clock and the carrier sources at the transmitter to be locked, a new method for estimating the clock frequency offset is explored which is independent of the carrier frequency offset.

In Chapter 4, algorithms are developed for the other critical blocks in the baseband receiver: namely the channel frequency response estimator, null tone detector and equalizer/diversity combiner. A proposal is outlined where the high throughput requirement of decoding a convolution encoded MBOFDM bit stream can be achieved by multiple parallel Viterbi decoders without significant performance degradation from using a single decoder (which would be able to maintain the channel state information continuously). Simulation studies are presented to characterize the performance of the whole baseband receiver in realistic UWB channels. We propose an alternate formulation for Dual Carrier Modulation (DCM), used for the 320/400/480 Mbps rates in [ECMA368], that is invariant to uncompensated cycle slips. An analytical framework is also developed for detecting narrow band victim services/interferers

through the available MBOFDM receiver. Finally alternate baseband receiver designs are explored that can work reliably in the presence of uncompensated IQ gain imbalance and quadrature skew, reducing the need for accurate calibration procedures in the analog front end of the transmitter and receiver.

In Chapter 5, mechanisms for enhancing the data rate/efficiency of MBOFDM transmission are explored beyond what is currently available as part of [ECMA368]. Schemes for increasing data rates in MBOFDM modems are developed by employing Multiple Transmit Receive antenna pairs and utilizing the frequency diversity that is naturally available in Multiband OFDM systems. We propose increasing the data rate to 600/640/720/800/960 Mbps without reducing the multiuser capacity of the network. A method is also proposed to reduce the overhead of the silent period after every MBOFDM symbol by 50% without any significant performance degradation. A mechanism for completely eliminating the silent period is explored when symbol hopping is employed the transmitter. Finally we use some of the proposals developed in this chapter to design a modulation structure that is robust to frequency dependent IQ Mismatch.

Major observations and comments are summarized in Chapter 6.